



## Amniotic Fluid-Derived Mesenchymal Stem Cells Prevent Fibrosis and Preserve Renal Function in a Preclinical Porcine Model of Kidney Transplantation

EDOUARD BAULIER,<sup>a,b</sup> FREDERIC FAVREAU,<sup>a,b</sup> AMÉLIE LE CORF,<sup>b,c</sup> CHRISTOPHE JAYLE,<sup>a,b</sup>  
FABRICE SCHNEIDER,<sup>b</sup> JEAN-MICHEL GOUJON,<sup>a,b</sup> OLIVIER FERAUD,<sup>c,d</sup> ANNELISE BENNACEUR-GRISCELLI,<sup>c,d</sup>  
THIERRY HAUET,<sup>a,b,e,\*</sup> ALI G. TURHAN<sup>b,c,d,\*</sup>

**Key Words.** Amniotic fluid-derived mesenchymal stem cells • Kidney transplantation • Pig • Preclinical model • Deceased after cardiac arrest donors • Ischemia reperfusion injury

### ABSTRACT

It is well known that ischemia/reperfusion injuries strongly affect the success of human organ transplantation. Development of interstitial fibrosis and tubular atrophy is the main deleterious phenomenon involved. Stem cells are a promising therapeutic tool already validated in various ischemic diseases. Amniotic fluid-derived mesenchymal stem cells (af-MSCs), a subpopulation of multipotent cells identified in amniotic fluid, are known to secrete growth factors and anti-inflammatory cytokines. In addition, these cells are easy to collect, present higher proliferation and self-renewal rates compared with other adult stem cells (ASCs), and are suitable for banking. Consequently, af-MSCs represent a promising source of stem cells for regenerative therapies in humans. To determine the efficiency and the safety of af-MSC infusion in a preclinical porcine model of renal autotransplantation, we injected autologous af-MSCs in the renal artery 6 days after transplantation. The af-MSC injection improved glomerular and tubular functions, leading to full renal function recovery and abrogated fibrosis development at 3 months. The strong proof of concept generated by this translational porcine model is a first step toward evaluation of af-MSC-based therapies in human kidney transplantation. *STEM CELLS TRANSLATIONAL MEDICINE 2014;3:809–820*

### INTRODUCTION

Ischemia/reperfusion (IR) is an unavoidable process acknowledged as being involved in acute and chronic kidney transplant dysfunction [1]. IR is characterized by a decrease in nutrients and oxygen supply during blood flow cessation, followed by oxidative stress injuries and inflammation after revascularization [2]. The main target of ischemic injury is the endothelial cell involved in hemodynamic instability, inflammatory cell recruitment, and tissue fibrosis leading to transplant dysfunction [3–5]. In this context, preventing or limiting the extension of vascular lesions due to IR is of the utmost importance [2, 3]. In kidney transplantation, the gradually increasing gap between the number of patients awaiting a transplant and the number of donors warrants the extension of eligibility criteria to include new donors such as donors deceased after cardiac arrest (DCDs). However, these organs are exposed to further injuries induced by warm ischemia [6, 7] and thus present a high rate of complications. Novel therapeutic strategies are required to improve organ function recovery following transplantation.

In this context, the use of stem cells to promote tissue repair is promising [8, 9]. Among the stem cells tested in regenerative medicine, amniotic fluid-derived mesenchymal stem cells (af-MSCs) seem particularly relevant [10]. These cells, obtained from amniotic fluid samples, are easy to isolate, have a high proliferation rate in vitro, can secrete proangiogenic and growth factors, and can differentiate into many cell lineages including renal cells [11–13]. af-MSCs have been reported to have beneficial effects in various ischemic and fibrotic situations, including kidney fibrosis in rodents [12, 14, 15]. A therapeutic approach involving af-MSCs as a stem cell-based therapy in organ transplantation would be relevant to promote graft function recovery and limit chronic organ dysfunction. However, the benefits of an af-MSC-based cell therapy remain to be demonstrated in a preclinical model of transplantation that is physiologically relevant to humans.

Given the anatomical differences between human and rodent kidneys, the translational impact of renal IR research performed in rats or mice is limited [16]. We developed a porcine model of kidney autotransplantation, allowing the study of graft outcome over long periods of time after

<sup>a</sup>INSERM U1082, Université de Poitiers, Faculté de Médecine et de Pharmacie, Poitiers, France; <sup>b</sup>CHU de Poitiers, Poitiers, France; <sup>c</sup>INSERM U935, Poitiers and Villejuif, France; <sup>d</sup>INSERM U935, Estem Pluripotent Stem Cell Core Facility and Ingestem Infrastructure, Université Paris Sud XI, Villejuif, France; <sup>e</sup>INRA, UE1372 GenESI, Plateforme Ibis, Surgères, France

\*Contributed equally to this work.

Correspondence: Thierry Hauet, M.D., Ph.D., INSERM U1082, 2 rue de la Miletirie, BP577, 86021 Poitiers Cedex, France. Telephone: 33-5-49-44-30-21; E-Mail: t.hauet@chu-poitiers.fr

Received October 18, 2013; accepted for publication March 10, 2014; first published online in *SCTM EXPRESS* May 5, 2014.

©AlphaMed Press  
1066-5099/2014/\$20.00/0  
<http://dx.doi.org/10.5966/sctm.2013-0186>

transplant [17]. The anatomical similarities (vascularization, size, multilobular and multipapillary organization) and physiological similarities (glomerular filtration, tubular functions) between porcine and human kidneys contribute to the major relevance of porcine models [17]. Moreover, we reported previously that combining 60 minutes of renal ischemia at body temperature with 24 hours of cold preservation in pigs induced kidney damage similar to that reported in human transplantation with DCDs [18].

In the *in vitro* part of the present study, we show that af-MSCs—collected in pigs at the end of gestation—are multipotent and protect endothelial cells from hypoxia/reoxygenation (HR) injuries. Moreover, af-MSCs are sensitive to HR *in vitro* and thus should not be injected during the preservation of kidney graft. We then demonstrate *ex vivo* and *in vivo* that af-MSC injection in renal artery improves their retention in the transplanted organ and limits their dissemination. Finally, we show *in vivo* that af-MSC injection in the renal artery 6 days after kidney autotransplantation strongly improves renal function recovery and prevents kidney fibrosis in a preclinical porcine model of poor graft quality, mimicking DCDs.

## MATERIALS AND METHODS

### Surgical Procedures

Surgical protocols were performed in accordance with the regional ethical committee for the use and care of laboratory animals (Committee no. 84, Agreements CE2012-4 and CE2012-29). A pregnant large white sow at 112 days of gestation (INRA du Magneraud, Surgères France, <http://www.poitou-charentes.inra.fr/en>) underwent caesarean section for piglet delivery. We took 10 ml of amniotic fluid from each piglet directly across the placental tissue, and the piglets were then collected. After one washing with AmnioChrome II medium (Lonza, Switzerland, <http://www.lonza.com>), cells were suspended in AmnioChrome II medium and plated in six-well culture plates at 37°C with 5% CO<sub>2</sub>, and the medium was subsequently replaced three times a week. After green fluorescent protein (GFP) marking, adherent cells were cryopreserved until injection. All cells used for experimentation were between passages 6 and 10. The day before transplantation, 3-month-old piglets were prepared as previously described [17]. Briefly, 1 hour of *in vivo* warm ischemia was induced in the left kidney by renal pedicle clamping. Next, the kidney was removed, cold flushed, and preserved at 4°C for 24 hours in UW solution (Bristol-Myers Squibb, New York, NY, <http://www.bms.com>). Twenty-four hours later, the left kidney was implanted into the same animal and the right kidney was removed. Six days after kidney transplantation, a saline solution (NaCl 0.9%) supplemented or not with autologous af-MSCs ( $1 \times 10^6$  cells per kilogram of body weight) was directly injected into the renal artery of the grafted kidney exposed by midventral laparotomy. We studied three groups of six animals with a 3-month follow-up: the vehicle group had injection of saline into the renal artery 6 days after kidney transplantation; the af-MSC group had injection of saline containing af-MSCs into the renal artery 6 days after transplantation (one more animal was injected with af-MSCs and sacrificed 24 hours after injection); and the control group had animals that underwent a uninephrectomy with no subsequent injection. All the animals underwent kidney biopsies at day 14 and month 1.

### Differentiation Studies

Before each experiment, af-MSCs were seeded ( $1 \times 10^6$  cells per well in 1 ml of AmnioChrome II medium) in six-well plates, as previously described [19]. For adipogenic differentiation, af-MSCs were cultured for 3 weeks using the human MSC (hMSC) Adipogenic BulletKit (Lonza), following the manufacturer's protocol. Oil Red O staining was used to detect adipocytes. For osteogenic differentiation, af-MSCs were cultured for 3 weeks using the hMSC Osteogenic BulletKit (Lonza), following the manufacturer's protocol. Differentiation was assessed by alizarin red S staining. Differentiation experiments were performed twice on two af-MSC lines. For each differentiation protocol, negative control conditions were achieved by culturing cells in AmnioChrome II medium. Supplemental data are available online.

### Phenotypic Analysis

All six af-MSC lines at passage 5 were tested for expression of mesenchymal stem cells markers: CD29, CD44 (1:10; BD Biosciences, San Diego, CA, <http://www.bdbiosciences.com>); CD73 (1:10; Santa Cruz Biotechnology Inc., Santa Cruz, CA, <http://www.scbt.com>); CD45, CD14 (1:50; AbD Serotec, Raleigh, NC, <http://www.abdirect.com>); CD105 (1:50; Novus Biologicals LLC, Littleton, CO, <http://www.novusbio.com>); SLA class II DR, CD90, CD34, c-kit (1:100; Abcam, Cambridge, U.K., <http://www.abcam.com>). A flow cytometry analyzer, FACSCanto II (BD Biosciences), was used.

### Coculture and Conditioned Media

Human aortic endothelial cells (HAECs) at passage 3 were cultured for 24 hours in a 24-well plate ( $8 \times 10^4$  cells per well) coated with 1% gelatin (Sigma-Aldrich, St. Louis, MO, <http://www.sigmaaldrich.com>) with EGM-2, Microvascular (EGM-2MV) medium (Lonza). After 24 hours of starvation in Endothelial Basal Medium (Lonza; starvation medium [SM]), cells underwent an HR sequence: 1 hour of hypoxia at 37°C in SM followed by 24 hours of cold hypoxia at 4°C in 150  $\mu$ l of UW solution (Viaspan; Bristol-Myers Squibb) in a chamber containing anoxic atmosphere (5% CO<sub>2</sub> and 95% N<sub>2</sub> [Bactal2; Air Liquide, France, <http://www.airliquide.com>]). Following hypoxia, HAECs were reoxygenated for 24 hours at 37°C in normoxic 5% CO<sub>2</sub> atmosphere according to three culturing protocols: coculture with af-MSCs in fresh SM, coculture with HAECs in fresh SM, and culture only in fresh EGM-2MV medium. For coculture conditions (protocols in fresh SM),  $1 \times 10^4$  cells (af-MSC passage 6 or HAEC passage 3) were seeded on 5- $\mu$ m-pore hanged cell culture inserts (Merck Millipore, Germany, <http://www.merckmillipore.com>) and placed in the wells of hypoxic HAECs. At the end of the procedure, conditioned media (af-MSC conditioned medium [ACM], HAEC conditioned medium [HCM], and EGM-2MV conditioned medium [ECM]) were collected, and we determined the percentage of living HR-treated HAECs at the bottom of the plates in each condition using trypan blue staining (supplemental online Fig. 2). Data are from three independent experiments (three af-MSC lines).

### Tube Formation Assay

HAECs at passage 3 were plated onto a 96-multiwell plate ( $2 \times 10^4$  cells per well) previously coated with 50  $\mu$ l of growth factor-reduced Matrigel (BD Biosciences). HAECs were cultured on Matrigel for 24 hours with 100  $\mu$ l of conditioned media from the coculture experiments described above (ACM, HCM, or

ECM). Tube network formation was assessed by counting the number of branch points and tubes in each well using Cella software (Olympus, Japan, <http://www.olympus-global.com>). Results are expressed with the ratio of each count in ACM or HCM conditions compared with the number observed in ECM (supplemental online Fig. 2). Data represented are from three independent experiments (three af-MSCLines).

### Cell Survival Experiments

af-MSCLines (passage 6) or HAECs (passage 3) were plated respectively in complete AmnioChrome II medium or complete EGM-2MV medium on 1% gelatin-treated 96-well plates ( $1.5 \times 10^4$  cells in 100  $\mu$ l of medium per well) for the 2,3-bis-(2-methoxy-4-nitro-5-sulfophenyl)-2H-tetrazolium-5-carboxanilide (XTT) experiment or 1% gelatin-treated 6-well plates ( $2 \times 10^5$  cells in 500  $\mu$ l of medium per well) for 7-aminoactinomycin D (7-AAD) viability staining. Cells were cultured for 12 hours at 37°C in a normoxic 5% CO<sub>2</sub> atmosphere. Hypoxia was then achieved by incubation of cells at 4°C in Viaspan solution in 5% CO<sub>2</sub> and 95% N<sub>2</sub> atmosphere. Reoxygenation was performed in SM for 24 hours at 37°C in normoxic 5% CO<sub>2</sub> atmosphere. Control cells were seeded in the same conditions as HR cells, but the 24-hour hypoxia and 24-hour reoxygenation phases were replaced by 48 hours of culture in SM at 37°C in normoxic 5% CO<sub>2</sub> atmosphere with medium replacement at 24 hours. We then used the XTT kit (Roche Applied Science, Indianapolis, IN, <https://www.roche-applied-science.com>) to assess cell viability, following the manufacturer's protocol. Results are expressed as percentage ratios of the absorbance (XTT) obtained in HR cells over absorbance of the same cells cultivated in control conditions. Cells were also stained for viability using the 7-AAD dye (BD Biosciences) and analyzed by flow cytometry. Data are from three independent experiments (three af-MSCLines).

### Lentiviral Transduction of the Six af-MSCLines

The day before transduction, porcine af-MSCLines at passage 4 were plated onto six-well plates ( $1 \times 10^5$  cells per well) in 2 ml of AmnioChrome II medium (Lonza) and incubated at 37°C in a 5% CO<sub>2</sub> atmosphere. Cells were transduced overnight with a VSV-G-pseudotyped TRIP lentivirus encoding for enhanced GFP under the control of an elongation factor 1 $\alpha$  promoter (kindly provided by Dr. Fabian Gross, CIC Biothérapies, Toulouse Hospital, Toulouse, France). Transductions were carried out at a multiplicity of infection of 5 in 1 ml per well of AmnioChrome II medium supplemented with 5  $\mu$ g/ml of protamine sulfate (MP Biomedicals, Irvine, CA, <http://www.mpbio.com>).

### Ex Vivo af-MSCLine Injection in a Preserved Kidney

We injected, ex vivo, a cellular suspension of one GFP-tagged af-MSCLine (passage 6,  $40 \times 10^6$  cells in 15 ml of NaCl 0.9%) directly into the artery of a kidney previously preserved for 24 hours in UW solution at 4°C. The cell suspension was infused over a 5-minute period and was followed by 10 minutes of washout with saline solution. Cryosections of large arteries and cortical tissue were performed and stained for GFP (1:100; Invitrogen, Carlsbad, CA, <http://www.invitrogen.com>).

### Renal Function Evaluation

Pigs were placed in a metabolic cage to allow specific 24-hour urine collections. Plasma and urinary creatinine, urinary proteins,

plasma, and urinary Na<sup>+</sup> were measured using an automated analyzer (Modular Analytics P; Roche). Blood and urinary osmolality were determined using a freezing-point depression technique.

### Immunohistochemical Studies

Three months after transplantation, frozen sections of kidney, liver, and lung tissue from euthanized animals were assessed for GFP (1:100; Invitrogen) and SWC3A (1:100; SouthernBiotech, Birmingham, AL, <http://www.southernbiotech.com>) expressions by immunofluorescence. All sections were examined under blind conditions by a pathologist and a nephrologist. Kidney biopsies were stained with the Periodic acid-Schiff (PAS) using a Leica ST5020 multistainer (Leica Biosystems, Wetzlar, Germany, <http://www.leicabiosystems.com>). Histological lesions were expressed using a previously described semiquantitative scale [17]: 0, no abnormality; 1, mild lesions affecting <10% of kidney samples; 2, lesions affecting 10%–25% of kidney samples; 3, lesions affecting 25%–50% of kidney samples; 4, lesions affecting 50%–75%; and 5, lesions affecting >75% of kidney samples. Paraffin sections were assessed for  $\alpha$ -smooth muscle actin expression ( $\alpha$ SMA; 1:50; Dako, Glostrup, Denmark, <http://www.dako.com>). Tissue sections were also labeled with Sirius Red staining [17]. The amount of  $\alpha$ SMA staining and Sirius Red coloration were determined by a semiquantitative imaging technique (Visilog 6.0; FEI Visualization Sciences Group, Burlington, MA, <http://www.vsg3d.com/visilog/overview>) on 10 different fields per slide and expressed as a percentage of the total surface area examined.

### Western Blotting

Three months after transplantation, pieces of snap-frozen kidney samples (cortex and outer medulla) were homogenized at 4°C in radioimmunoprecipitation assay lysis buffer. Protein extracts were separated on 12% sodium dodecyl sulfate polyacrylamide gel electrophoresis and transferred to a polyvinylidene difluoride membrane. Staining was performed with specific antibodies (Santa Cruz Biotechnology) against transforming growth factor- $\beta$  (TGF- $\beta$ ; 1:600), vascular endothelial growth factor (VEGF) A (1:100), VEGF receptor 1 (Flt1; 1:100), or angiotensin-1 (Ang1; 1:100). Proper secondary antibodies, conjugated to horseradish peroxidase (GE Healthcare, Little Chalfont, U.K., <http://www.gehealthcare.com>), were used to reveal the labeled bands (ECL kit; GE Healthcare).  $\beta$ -Actin was used for normalization (1:40,000; Sigma-Aldrich). Intensities of the protein bands were determined and quantified using AlphaEase FC software (Alpha Innotech, San Leandro, CA, <http://www.alphainnotech.com>).

### Enzyme-Linked Immunosorbent Assay

Concentrations of plasma TGF- $\beta$  were quantified on blood samples using a quantitative sandwich enzyme-linked immunosorbent assay kit (R&D Systems Inc., Minneapolis, MN, <http://www.rndsystems.com>).

### Statistical Analysis

Results are expressed as mean  $\pm$  SEM. Because the experimental groups each contained six animals, we performed a nonparametric Mann-Whitney test for two-group comparisons. When three groups were analyzed, we used the Kruskal-Wallis test with Dunn's multiple comparisons test. When groups contained fewer than six animals, we performed an unpaired nonparametric

*t* test with Welch correction. For intragroup comparisons, we applied Wilcoxon's test. All statistical analyses were performed with the GraphPad InStat software (GraphPad Software, Inc., San Diego, CA, <http://www.graphpad.com>). *p* values <.05 were considered significant.

## RESULTS

### af-MSc Characterization

To characterize the af-MSCs collected at birth, we tested their phenotype and their differentiation properties. Porcine af-MSCs exhibited differentiation properties similar to MSCs, in particular the differentiation into adipocyte as shown by Oil Red O staining (Fig. 1A) and into osteoblasts with positive alizarin red S staining (Fig. 1B). In our experiments, af-MSCs highly expressed MSC markers CD90, CD73, CD44, and CD29, whereas they had low expression of CD105, CD14, SLA class II DR, CD34, CD45, and stem cell factor receptor c-kit (CD117) (Fig. 1C). In addition, af-MSCs poorly differentiated into endothelial cell lineage (supplemental online Fig. 1).

### In Vitro Protective Effects of af-MSCs on Endothelial Cells

Because IR injury (IRI) especially targets endothelial cells, it was important to assess the potential of af-MSCs to protect these cells against IRI. We reproduced organ-preservation conditions in an *in vitro* model. In this model, the introduction of af-MSCs during the reoxygenation step in a culture insert (coculture without direct contact) significantly increased survival of endothelial cells, as assessed by trypan blue staining (Fig. 2A). This led us to perform functional experiments to assess the possible induction of proangiogenic factor secretion by af-MSCs in a posthypoxic microenvironment. We collected coculture media at the end of reoxygenation in two experimental conditions: af-MSCs cocultured with hypoxic HAECs and HAECs cocultured with hypoxic HAECs (supplemental online Fig. 2). Conditioned media from af-MSCs cocultured with hypoxic HAECs (ACM) added to HAECs incubated on growth factor-reduced Matrigel and induced more capillary-like structures than conditioned media from HAECs cocultured with hypoxic HAECs (HCM), as shown by the significantly higher number of tubes and branch points per well (Fig. 2B). Values obtained with the coculture-conditioned media were compared with values obtained with HAECs cultured onto Matrigel in optimal endothelial cell culture medium (ECM).

### In Vitro Sensitivity of af-MSCs to HR

Injection of af-MSCs during the *ex vivo* preservation phase of kidney grafts could be therapeutically valuable because the injected cells would not be captured by untargeted organs; however, this injection protocol would expose af-MSCs to a hypothermic ischemic environment, leading to massive cell death if these cells are sensitive to IRI. To assess the sensitivity of af-MSCs to IR sustained during transplantation, we exposed the cells to a combination of hypoxia at low temperature in organ-preservation solution and reoxygenation. We used HAECs known to be very sensitive to *in vivo* IR as a positive control of high HR sensitivity. At the end of reoxygenation, af-MSCs showed the same low XTT cleavage activity and poor cell viability as assessed by positive staining for 7-AAD as HAECs. These results strongly suggest that af-MSCs are sensitive to IR (Fig. 3A).

### Ex Vivo and In Vivo af-MSc Tracking

Cell tracking after injection is one of the critical steps of studies on stem cell therapy because ectopic engraftment of cells could be associated with possible complications. Because of our long period of follow-up, we chose to label af-MSCs with GFP by lentiviral transduction to achieve long-term transgene expression. The mean percentage of GFP-positive cells was 44%. Our next step was to validate (*ex vivo*, then *in vivo*) the feasibility of our injection protocol. We injected GFP-positive af-MSCs in the renal artery of a preserved kidney. After 10 minutes of washout with saline solution, we found GFP-positive cells on the luminal surface of arteries and trapped in glomeruli, as shown in Figure 3B. We did not detect any GFP-positive cells by flow cytometry in the washing solution flowing out of the vein. This finding suggests that direct injection of af-MSCs in renal artery allowed optimal delivery of cells within the kidney with a minimal risk of dissemination and without evidence of kidney vasculature obstruction. After having established the feasibility of our injection protocol *ex vivo*, we wanted to assess *in vivo* whether af-MSc injection via the renal artery could prevent dissemination of the cells to other organs shortly after injection; therefore, we sacrificed one transplanted animal 24 hours after af-MSc injection. GFP-positive cells were detectable within the kidney both on the luminal surface of arteries and in the interstitial space (Fig. 4A, 4B; gray arrows). We did not find GFP-positive cells in the lungs, the spleen, or the liver 24 hours after injection (supplemental online Fig. 3). In the group of animals sacrificed at the end of follow-up, we detected GFP-positive cells in the transplanted kidneys in only two animals, as shown in Figure 4C (gray arrows). GFP-positive cells were not detected in transplanted kidneys of the other four animals from the af-MSc group (Fig. 4D). Moreover, we did not find GFP-positive cells in the lungs, the spleen, or the liver of any af-MSc-treated animals at 3 months after transplantation (supplemental online Fig. 3).

### Effects of af-MSCs on Renal Transplant Function and Tissue Integrity

To assess the therapeutic benefits of af-MSc injection, we evaluated renal function recovery in pigs by monitoring serum creatinine levels before and after treatment (Fig. 5). Serum creatinine levels of healthy animals that did not undergo surgery usually did not exceed a value of  $88 \pm 3 \mu\text{M}$  ( $n = 10$ , data not shown). In both surgical groups, we observed an increase in serum creatinine levels up to  $1,000 \mu\text{M}$  due to IR injuries following kidney transplantation from DCD conditions. Creatininemia remained similar between groups in the first 11 days after transplantation; however, 7 days after af-MSc injection (14 days after transplantation), creatininemia dropped back to pretransplant levels ( $90 \pm 3 \mu\text{M}$ ) and remained stable until the end of follow-up. In contrast, vehicle-treated animals presented high levels of serum creatinine ( $251 \pm 4 \mu\text{M}$ ) from day 14 until the end of follow-up. Finally, proteinuria, which attests to glomeruli integrity, was significantly lower in the af-MSc group compared with the vehicle group (Fig. 6A).

To complete our investigations on transplanted kidney function, we performed graft histological analysis. PAS staining on cortex biopsies performed at day 14 and month 1 showed that af-MSc injection significantly preserved the integrity of tubule brush borders. Moreover, swine injected with af-MSCs exhibited reduced levels of tissue-infiltrated cells and a decrease in tubular

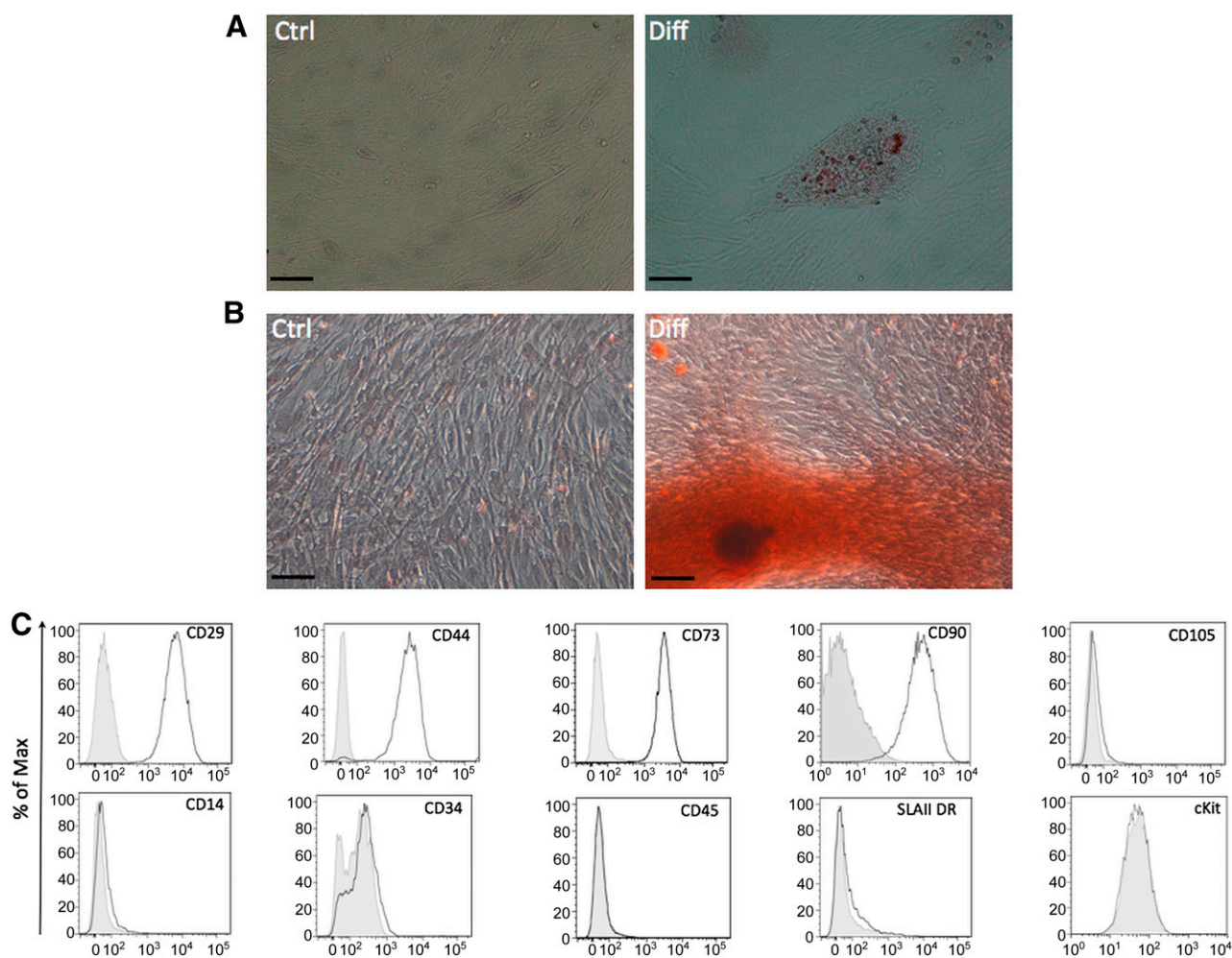


**Figure 1.** Characterization of porcine amniotic fluid-derived mesenchymal stem cells (af-MSCs) obtained at the end of gestation. **(A):** af-MSCs differentiated into adipocyte-like cells, as marked by Oil Red O staining. **(B):** af-MSCs differentiated into osteoblast-like cells, as indicated by alizarin red staining. Scale bars = 50  $\mu$ m. **(C):** Mesenchymal stem cell markers CD29, CD90, CD73, CD44, CD105, CD14, SLA class II DR, CD34, CD45, and stem cell factor receptor (c-kit) expression on af-MSCs shown by flow cytometry analysis of undifferentiated cells. Solid gray lines are isotype controls. Abbreviations: Ctrl, control; Diff, differentiated; SLAII DR, SLA class II DR.

epithelial cell detachment, which was particularly severe in vehicle-treated animals (Fig. 6B). Renal tissue integrity of animals from the af-MSC group was similar to native kidneys obtained from animals subjected to single nephrectomy (control group; data not shown), supporting full tubular function recovery. Indeed, after af-MSC injection, the decrease in sodium excretion fraction was associated with an increase in the urine-to-blood osmolarity ratio, suggesting good recovery of the reabsorption function of the kidney after transplantation (Fig. 6C).

#### Effects of af-MSCs on SWC3A-Positive-Cell Recruitment and Fibrosis Development

Transplanted kidneys from the af-MSC group demonstrated significant reduction of collagen production and myofibroblast infiltration within the interstitial space in the cortex as shown by quantification of the Sirius Red and  $\alpha$ SMA staining of kidney samples at 3 months after transplantation (Fig. 7A). SWC3A is a marker mostly present on the surface of porcine macrophages. Quantification of SWC3A-positive cells in kidneys showed that af-MSC-treated pigs had fewer infiltrated cells (Fig. 7A). This finding

was associated with a significant reduction in tubular atrophy revealed by PAS staining on the cortex section at 3 months after transplantation (Fig. 7A).

#### Modulation of Growth Factor Expression Following af-MSC Injection

In order to further investigate the role of af-MSCs in renal function recovery and fibrosis reduction, we assessed the activation status of proangiogenic and profibrotic pathways (Fig. 7B, 7C). We observed that af-MSC injection at 6 days after transplantation promoted, 3 months later, higher levels of VEGFA and Ang1 in kidneys. Interestingly, expression of Flt1 was downregulated in kidneys of af-MSC-treated pigs.

To investigate the kinetics of activation of the TGF- $\beta$  signaling pathway during the postinjection period, we evaluated TGF- $\beta$  plasma levels. Circulating TGF- $\beta$  levels were significantly more elevated 24 hours after injection of af-MSCs compared with vehicle injection (Fig. 7C). However, cortical TGF- $\beta$  levels in kidney grafts at 3 months after transplantation were similarly elevated in all transplanted experimental groups (Fig. 7C).

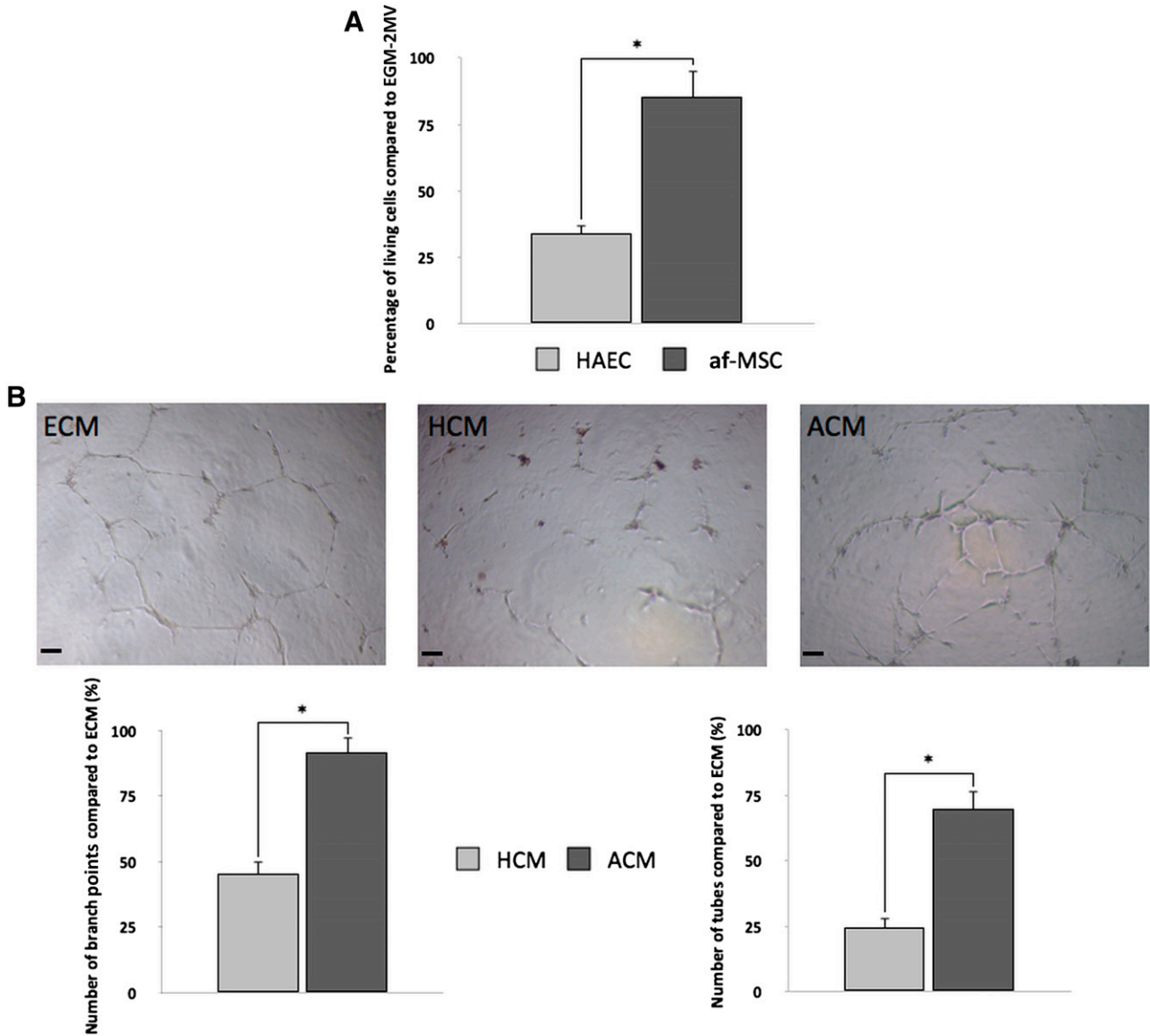


**Figure 2.** af-MSCs enhance survival and plasticity of HAECs after hypoxia/reoxygenation. **(A):** Number of living HAECs after hypoxia and coculture with af-MSCs or HAECs during reoxygenation assessed by trypan blue staining. **(B):** Tubular structure sprouting of HAECs in HCM or ACM by counting number of branch points and number of tubes per well and representative pictures. Scale bars = 400 μm. Abbreviations: ACM, af-MSC-conditioned medium; af-MSC, amniotic fluid-derived mesenchymal stem cell; ECM, EGM-2MV-conditioned medium; EGM-2MV, EGM-2 microvascular medium; HAEC, human aortic endothelial cell; HCM, HAEC-conditioned medium.

**DISCUSSION**

In experimental studies, most af-MSCs are isolated at an early or middle stage of gestation by amniocentesis or after sacrifice of the fetus [12, 13, 19, 20]. In our porcine model, it was impossible to collect af-MSCs at an early stage without sacrificing the piglet. Because MSCs are not immunologically privileged, and because we chose to investigate af-MSC therapy without an allo-recognition phenomenon (autologous cell therapy), we collected the autologous af-MSCs just before birth, during piglet delivery by caesarean section. Our first concern was to determine whether af-MSCs isolated at birth had the same stem cell potential described in human cells [13, 19] by testing their phenotype and their differentiation capabilities. Isolated porcine af-MSCs could be differentiated into adipocyte and osteoblast lineages,

consistent with the results of previous studies [19, 21, 22]. However, our differentiation experiments suggest that the differentiation potential of af-MSCs collected at the end of gestation could be slightly lower than the af-MSCs isolated at an early stage of gestation, particularly for endothelial cell differentiation. This observation is consistent with recent findings on af-MSCs isolated from human third-trimester amniotic fluid [13, 20].

In our experiments, af-MSCs highly expressed the CD90, CD29, CD44, and CD73 surface markers but not the CD14, CD34, CD45, and SLA class II DR surface markers, and this is consistent with an MSC profile. Surprisingly, CD105 expression was low on af-MSCs collected at the end of gestation. This is in accordance with a previous report demonstrating modulation of the expression of some MSC markers on af-MSCs in relation to the time of gestation [23]. However, the phenotypic pattern described

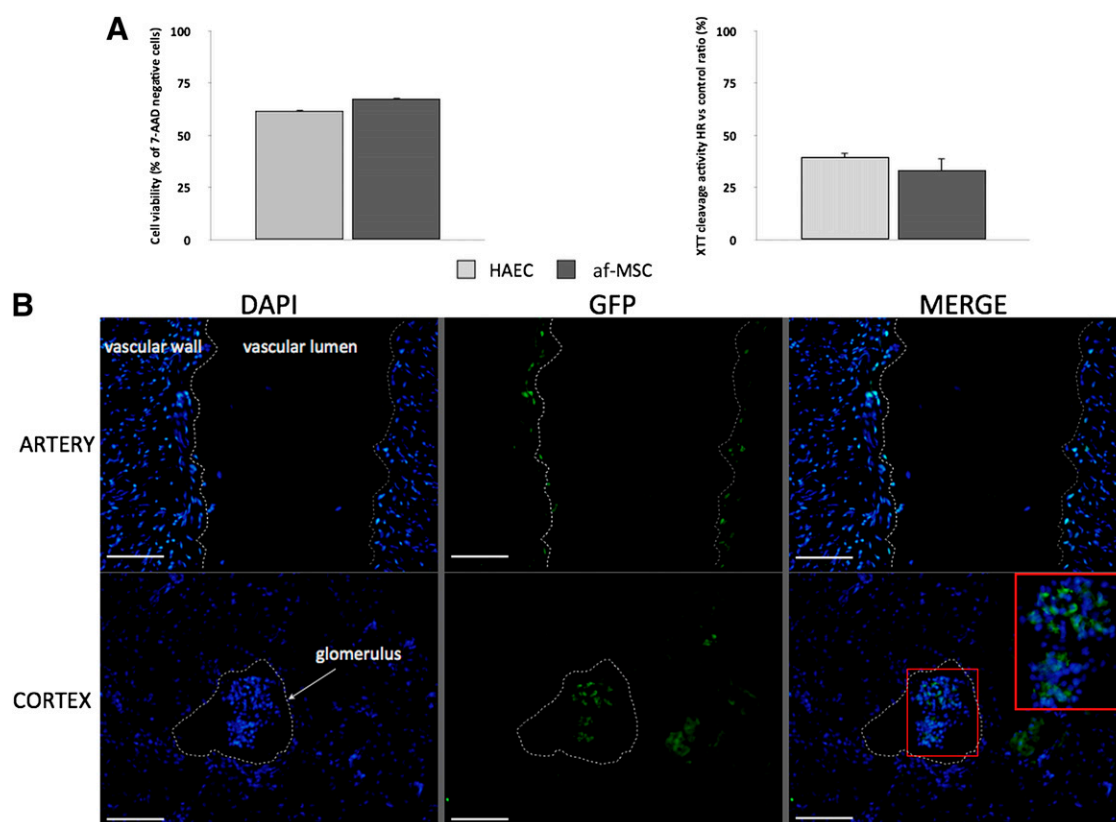


**Figure 3.** af-MSCs are sensitive to HR in vitro and are trapped within the kidney after ex vivo injection in renal artery. **(A):** Representation of 7-AAD viability staining by flow cytometry analysis and XTT cleavage activity of af-MSCs and HAECs after HR sequence compared with normoxic conditions. **(B):** GFP staining on artery and cortex cryosections of preserved kidney after ex vivo injection of GFP-tagged af-MSCs. Glomerulus and vascular structures are highlighted with white dashed lines. Scale bars = 100  $\mu$ m. Abbreviations: 7-AAD, 7-aminoactinomycin D; af-MSC, amniotic fluid-derived mesenchymal stem cell; DAPI, 4',6-diamidino-2-phenylindole; GFP, green fluorescent protein; HAEC, human aortic endothelial cell; HR, hypoxia/reoxygenation; XTT, 2,3-bis-(2-methoxy-4-nitro-5-sulphophenyl)-2H-tetrazolium-5-carboxanilide.

by other MSC markers follows the International Society for Cellular Therapy recommendations for MSC definition [24]. In the present work, stem cell factor receptor c-kit was expressed by only 1% of the af-MSCs. Although most previous studies were performed with c-kit-positive-sorted af-MSCs, recent work showed that c-kit-positive and c-kit-negative af-MSCs mostly share the same differentiation potential, except that for myocardial differentiation [25]. Consequently, we selected af-MSCs by direct adhesion because this method is suitable for clinical application and avoids cell sorting, which is expensive and time consuming.

af-MSCs are known to secrete cytokines, growth factors, chemoattractive molecules, and remodeling enzymes. Prosurvival effects of af-MSCs in other ischemic pathologies are probably due to secretion of a combination of these factors [12–16]. To assess whether end-term porcine af-MSCs isolated by adhesion could protect endothelial cells from IR and/or preserve their capability to form tubes after IR via secretion of soluble factors, we cocultured, without direct contact, af-MSCs with HAECs subjected to an in vitro HR sequence mimicking in vivo transplantation. Coculturing unstressed af-MSCs with HAECs subjected to HR is a relevant experimental design to mimic organ transplantation because unstressed af-MSCs administered as a cellular therapy after kidney transplantation would meet stressed or damaged endothelial cells as possible targets. This experimental design demonstrated that af-MSCs promoted both HAEC survival after HR and tube formation. Although these in vitro results cannot be

fully extrapolated to the in vivo condition, the data obtained strengthen the hypothesis that af-MSCs might have a beneficial impact on endothelial IR injuries following kidney transplantation through secreted factors.

In renal transplantation, a potential route of delivery of af-MSCs to the kidney would be direct injection of the cells into the renal artery during cold preservation [26]. However this may reduce the viability of af-MSC because of the deleterious microenvironment linked to IR. We confirmed this in vitro, showing that af-MSCs were sensitive to the conditions of organ preservation (hypoxia, low temperature, and preservation solution), thus excluding af-MSC administration during kidney preservation. Consequently, we chose to inject af-MSCs 6 days after transplantation to avoid the direct effects of the IR sequence but still to administer the cells during the course of the regenerative processes, which our own work showed starting 3 days after transplantation [18]. Moreover, we decided to inject cells in the renal artery to avoid the systemic dissemination associated with intravenous injection in rodent models [9, 12]. We chose to tag the cells by lentiviral transduction inducing GFP expression for long periods of time (more than 3 months) and to assess GFP expression by immunodetection in large biopsy, allowing screening from different parts of each organ. This protocol is of great interest for detecting remnant stem cells injected in large-animal models, such as the pig, with human size organs. In preliminary homing experiments, GFP-positive af-MSCs were detectable in the kidney

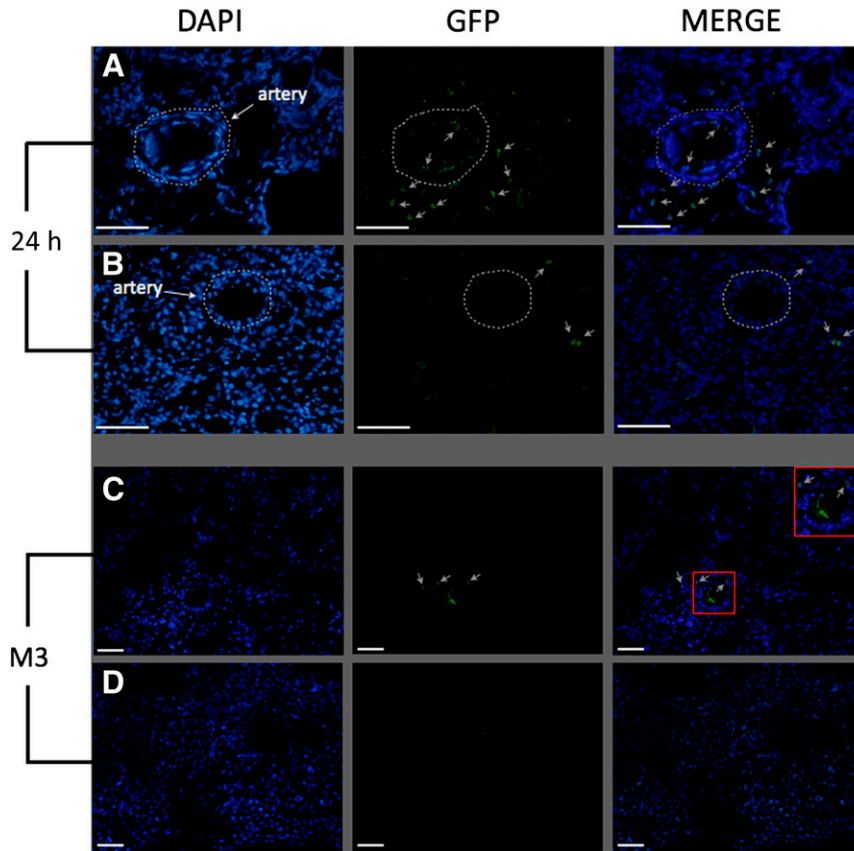


**Figure 4.** Amniotic fluid-derived mesenchymal stem cells (af-MSCs) are found in the kidney 24 hours and 3 months after injection. GFP staining on cryosections of renal cortex 24 hours (A, B) and 3 months (C, D) after injection of GFP-marked af-MSCs in vivo. Animals with (C) or animals without (D) detectable GFP-positive cells in kidney grafts 3 months after af-MSC injection. Scale bars = 100 μm. Gray arrows: positive cells. White dashed lines: arteries. Abbreviations: DAPI, 4',6-diamidino-2-phenylindole; GFP, green fluorescent protein; h, hour; M3, month 3.

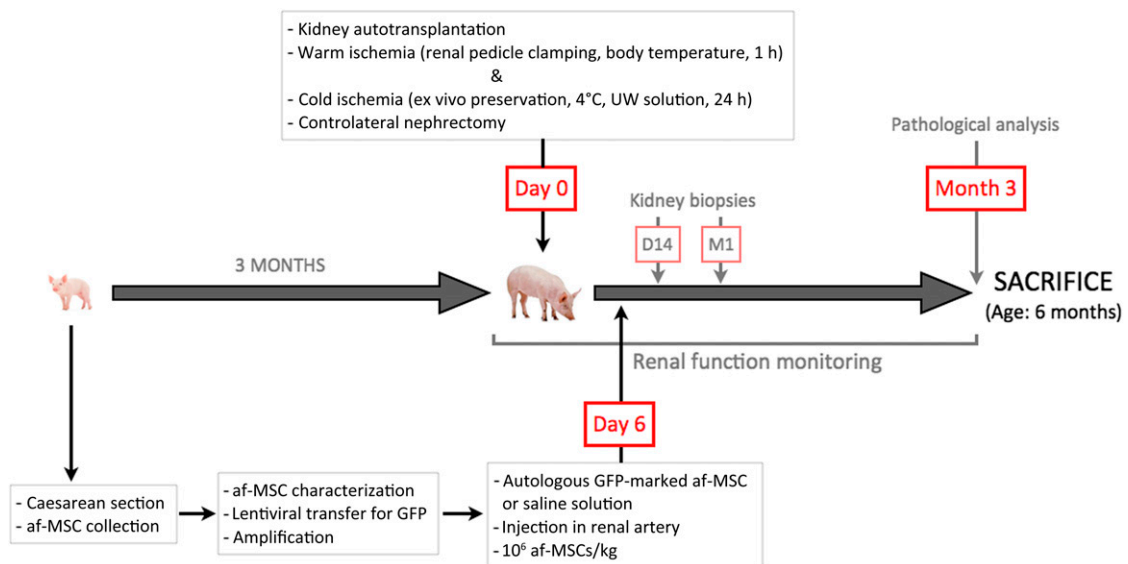


**Figure 5.** Schematic representation of the study progression. Abbreviations: af-MSC, amniotic fluid-derived mesenchymal stem cell; D, day; GFP, green fluorescent protein; h, hour; M, month.

10 minutes after ex vivo injection or 24 hours after in vivo injection in a transplanted kidney. After injection into the renal artery, numerous af-MSCs were localized close to the endothelium and within renal interstitial tissue, demonstrating their high retention

rate in the targeted kidney. This was associated with an absence of dissemination because there were no detectable GFP-positive cells in nontargeted organs at 24 hours and 3 months after injection. GFP-expressing cells were found only in two of six renal



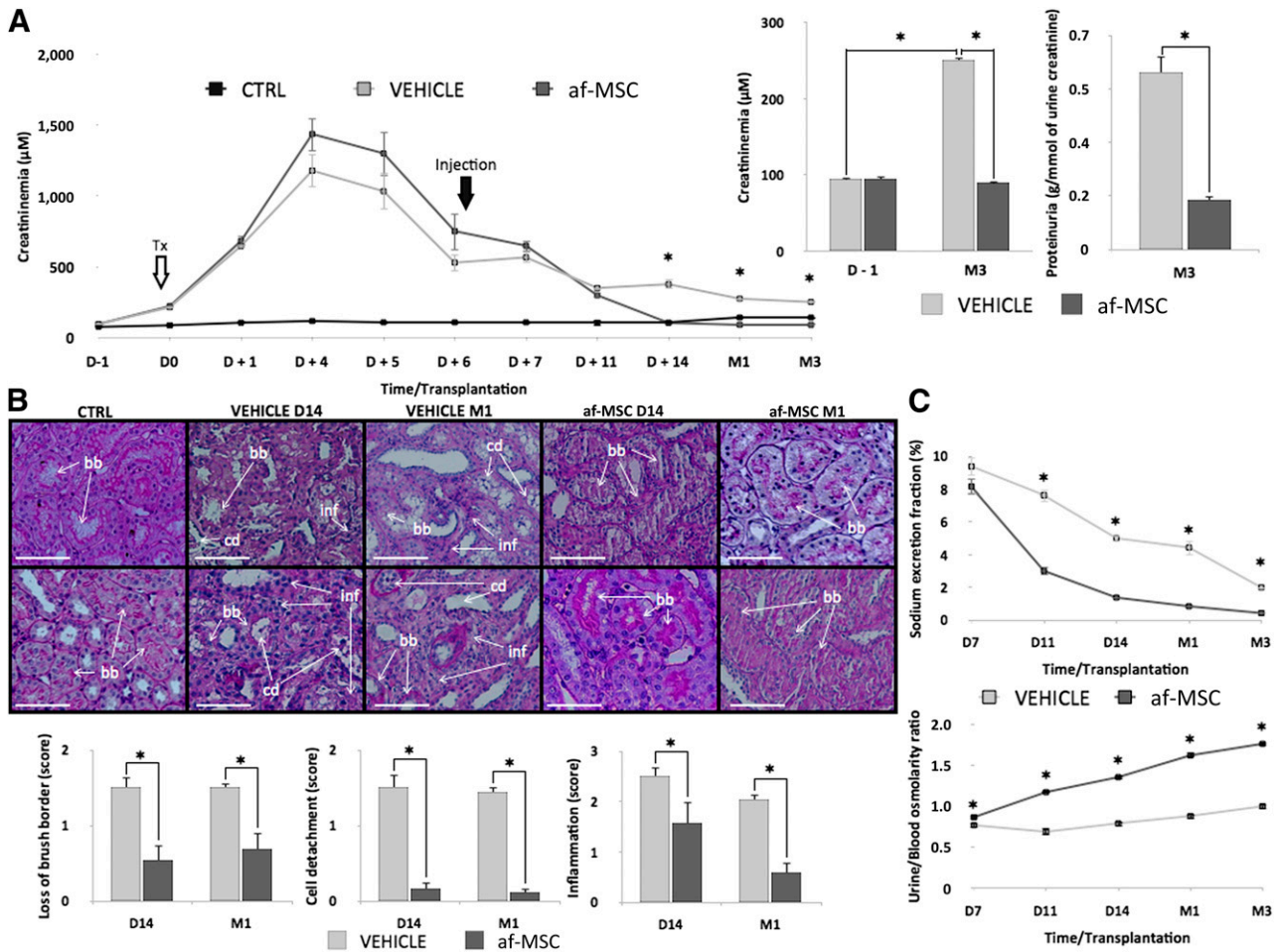


**Figure 6.** af-MSC injection significantly improved tissue healing and renal function recovery. **(A):** Plasma creatinine levels measured during 3 months of follow-up of af-MSC-treated, vehicle-treated, and uninephrectomized (control) animals and proteinuria levels from vehicle and af-MSC groups at the end of follow-up (3 months after transplantation). **(B):** Periodic acid-Schiff staining on kidney biopsies collected 2 weeks and 1 month after transplantation. Histological scores of tubules brush border loss, cell detachment, and tissue inflammation. Pictures are from different animals. Scale bars = 100 μm. **(C):** Tubular function assessment by sodium excretion fraction levels and calculated urine/blood osmolarity ratio from D7 to M3 following transplantation. Abbreviations: af-MSC, amniotic fluid-derived mesenchymal stem cell; bb, brush border; cd, cell detachment; CTRL, animal with native kidney; D, day; inf, tissue inflammation; M, month.

grafts and remained undetectable in other organs, suggesting elimination of most of the af-MSCs from the kidney. Indeed, we can hypothesize that af-MSCs fail to engraft efficiently in the long term and that most are eliminated from the body by 3 months after injection. The poor differentiation in vitro into endothelial cells of end-term porcine af-MSCs, associated with their poor long-term engraftment in the transplanted kidney after injection, suggests that af-MSCs are unlikely to induce tissue regeneration by in situ differentiation and direct cell replacement.

After having characterized porcine af-MSCs collected at the end of gestation, established in vitro the reparative potential of af-MSCs on stressed endothelial cells, and assessed ex vivo and then in vivo the protocol of af-MSC injection, our next step was to determine a proof of concept of the benefits of af-MSC injection after transplantation. We used a porcine model of IR combining 1 hour of warm ischemia and 24 hours of ex vivo static cold preservation before autotransplantation. This sequence, similar to the one present with DCDs, induces severe damage with poor graft survival [17]. Kidney function analysis showed that the therapeutic effect of af-MSC injection compared with saline infusion

became clear at day 14 (7 days after injection) and persisted during the 3-month follow-up.

Furthermore, in the af-MSC-treated animals, we highlighted a fast decrease in sodium excretion fraction associated with an increase in the osmolarity ratio, both reaching basal levels early after injection of af-MSCs. This suggests fast recovery of reabsorption functions of the graft and was not observed in the vehicle group. These results were supported by the anatomopathological studies performed on early kidney biopsies demonstrating that af-MSC injection increased tubule regeneration and limited tubular epithelium detachment and tissue inflammation. At month 3, the reduction of tubular atrophy observed in the af-MSC group was associated with a drastic decrease in proteinuria. These considerations are important because IR lesions are unavoidable in kidney transplantation and generate extensive kidney fibrosis, leading to kidney dysfunction and graft loss [1, 4, 5]. In addition, af-MSC injection prevented fibrosis development. Fibrosis is linked to chronic interstitial infiltration by leukocytes [27], and we observed a significant reduction in renal infiltrated SWC3A-positive cells in the af-MSC group. SWC3A is mainly

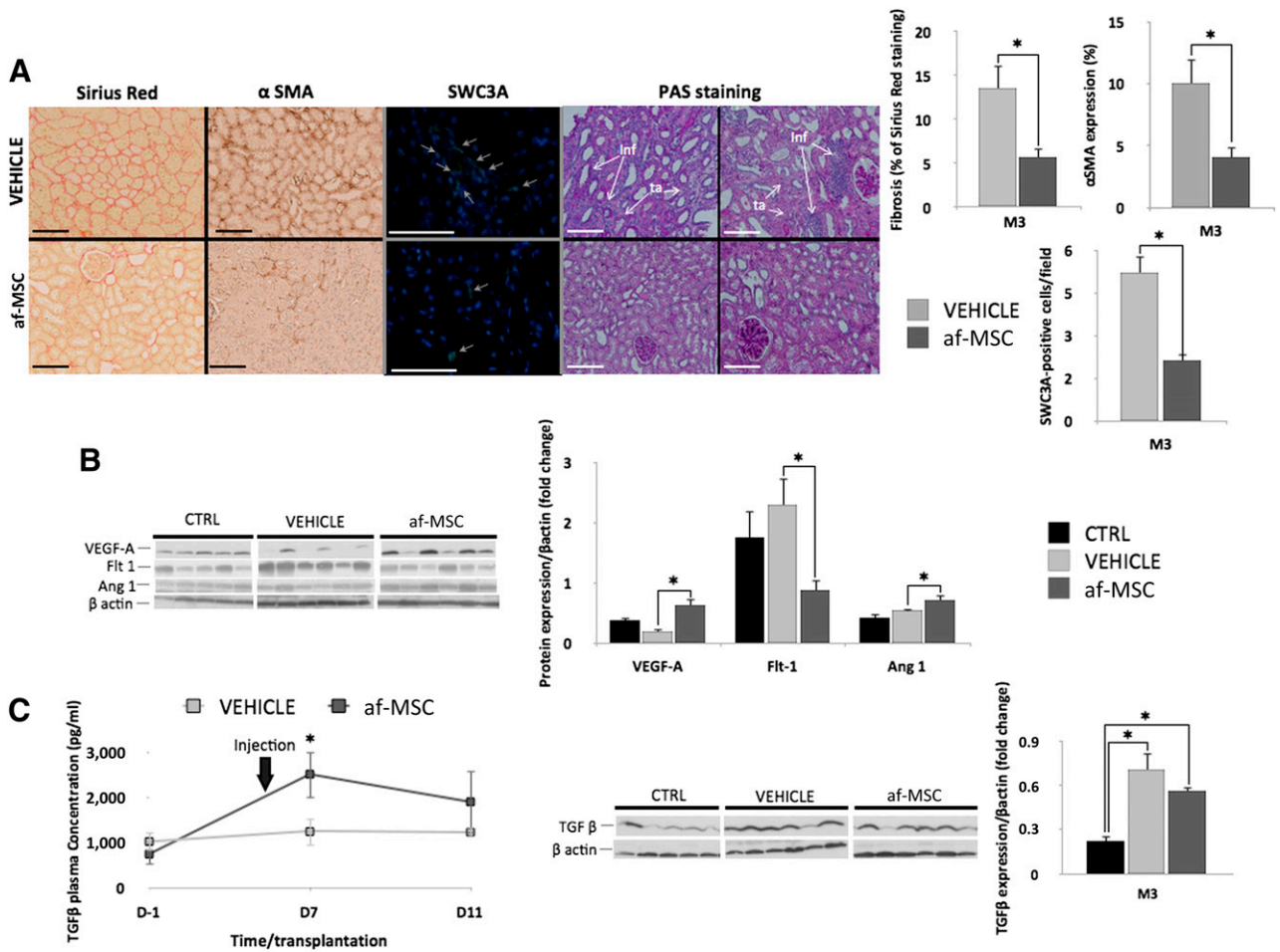


**Figure 7.** af-MSC injection efficiently prevented tissue fibrosis, SWC3A-positive-cell recruitment, and tubular damage and induced expression levels of proangiogenic growth factors. **(A):** Sirius Red,  $\alpha$ SMA, SWC3A, and PAS staining performed on kidney sections at 3 months after transplantation and their quantitative representations. Scale bars = 100  $\mu$ m. Gray arrows: positive cells. Each picture is from a different animal. **(B):** Western blot analysis and quantitative representations of VEGFA, Flt1, and Ang1 expression in kidneys of uninephrectomized (control), vehicle-treated, and af-MSC-injected pigs at 3 months after transplantation. **(C):** Enzyme-linked immunosorbent assay quantification of TGF- $\beta$  in plasma of pigs from vehicle and af-MSC groups, followed by Western blot analysis and quantitative representation of TGF- $\beta$  expression in kidneys of uninephrectomized (control), vehicle-treated, and af-MSC-injected pigs at 3 months after transplantation. \*,  $p < .05$ . Abbreviations:  $\alpha$ SMA,  $\alpha$ -smooth muscle actin; af-MSC, amniotic fluid mesenchymal stem cell; Ang1, angiotensin 1; CTRL, animal with native kidney; Flt1, VEGF receptor 1; PAS, Periodic acid-Schiff; TGF- $\beta$ , transforming growth factor  $\beta$ ; VEGFA, vascular endothelial growth factor A.

expressed by macrophages [28]. This result suggests that the immune modulation activity of af-MSCs could have been focused on the innate immune system and especially on macrophages. These findings suggest that af-MSCs may have at least two possible protective mechanisms of action, either by promoting renal cell survival after IR injuries, including endothelial cells, or by modulating macrophages recruitment and consequently reducing inflammation and fibrosis.

To determine the mechanisms involved in the protective effects of af-MSC injection on the renal endothelium, we subsequently explored the proangiogenic pathways involved in tissue healing after IR. Blots performed 3 months after transplantation suggested that af-MSC injection contributed to the activation and maintenance of angiogenesis in ischemia-injured kidneys, as shown by significant increases in VEGFA and Ang1 expression in kidneys from the af-MSC group. Assessing both parameters is of particular interest because VEGFA is described as a major proangiogenic growth factor, inducing endothelial cell survival

and proliferation as well as formation of a new vascular network [29–31], whereas Ang1 has been shown to be involved in capillary structure strengthening and maintenance of vessel stability and is secreted chronologically after VEGF during the angiogenic reparative processes triggered by IR damage [30, 32].

The physiological role of Flt1 remains controversial, but it is suspected that Flt1 is a decoy VEGFA receptor [33–35] that could negatively regulate angiogenic signaling. Western blot analysis revealed a significant decrease in Flt1 expression in af-MSC-treated kidney grafts, suggesting a potential enhancement of the proangiogenic activity of VEGFA. Moreover, inflammatory cells such as macrophages express Flt1. This observation could be consistent with the concomitant decrease in SWC3A-positive-cell infiltration in these kidneys. Taken together, these results strongly suggest the establishment of a proangiogenic microenvironment for up to 3 months after kidney transplantation in swine injected with af-MSCs. These cells can secrete VEGFA and Ang1 [12, 21], but the exact cell types involved in this production

in the kidney at the end of follow-up remain unknown. Because of the low number of GFP-positive af-MSCs observed in the graft at month 3, we hypothesize that af-MSCs might be involved indirectly in this phenomenon by promoting, at the time of injection, regenerative processes that are still active 3 months later.

TGF- $\beta$  is a cytokine involved in cell differentiation, proliferation, and apoptosis. TGF- $\beta$  can have beneficial effects at the early stages of regenerative processes, but chronic high levels of TGF- $\beta$  promote collagen production and epithelial-to-mesenchymal transition, enhancing fibrosis development and graft loss [35, 36]. In a proangiogenic environment, TGF- $\beta$  induces endothelial cell proliferation and migration, promotes neovessel stabilization, and tends to inhibit inflammatory cell adhesion and transmigration across the endothelium [37–39]. TGF- $\beta$  also promotes the commitment of CD4<sup>+</sup> T cells toward the induced regulatory T-cell lineage that could protect kidney grafts [38–40].

We decided to investigate the kinetics of TGF- $\beta$  levels in peripheral blood following af-MSC injection because kidney biopsies are too small for Western blot analysis. Plasma levels of TGF- $\beta$  were transiently higher in af-MSC-treated animals immediately after cell injection (day 7) and reached similar levels in both groups at day 11. This was associated, 3 months after transplantation, with similar increases in cortical levels of TGF- $\beta$  in the vehicle- and af-MSC-treated groups. The extensive renal fibrosis found in the vehicle group suggests that the early and transient increase in systemic TGF- $\beta$  levels in the af-MSC-treated animals could be beneficial or that af-MSCs prevent fibrosis development via secretion of unidentified antifibrotic substances.

## CONCLUSION

This preclinical DCD porcine model demonstrates the feasibility and the beneficial effects of an af-MSC-based cell therapy by promoting kidney function recovery after transplantation. Compared with other adult stem cells, af-MSCs are easy to collect when amniotic fluid is sampled at the end of gestation and exhibit higher proliferative rate without obvious DNA damage associated with cell growth [41]. Consequently, one donor could generate doses for multiple patients, making af-MSCs a therapeutically valuable

source of stem cells suitable for banking for various indications in human medicine, such as induction of tissue regeneration in kidney transplantation. Moreover, clinical applications of stem cell technology require preclinical studies in large animals to validate therapies that have been identified in small-animal models and to reduce the risk of testing an ineffective therapy in humans [42]. In this context, the highly translational porcine model used for this study is a powerful tool to assess the safety and feasibility of stem cell-based therapies in the field of solid organ transplantation.

## ACKNOWLEDGMENTS

We are grateful to Nicolas Chatauret, Raphael Thuillier, and Sebastian Giraud for their guidance and advice; Sandrine Joffrion and Marie-Laure Bonnet for their excellent technical assistance with the in vitro experiments; Pierre-Olivier Delpech, William Hebrard, and Thibaud Saint-Yves for their efficient implementation of surgery procedures; and Tackwa Khalifeh and Paul Roblot for their helpful work performed during the course of their master's studies. This work has benefited from the facilities and expertise of the ImageUP platform (Institut de Physiologie et Biologie Cellulaires—University of Poitiers).

## AUTHOR CONTRIBUTIONS

E.B. and F.F.: conception and design, provision of study material, collection and/or assembly of data, manuscript writing, final approval of manuscript; A.L.C.: provision of study material, final approval of manuscript; C.J., F.S., O.F.: provision of study material; J.-M.G.: provision of study material, collection and/or assembly of data; A.B.-G.: financial support, administrative support; T.H.: conception and design, provision of study material, collection and/or assembly of data, data analysis, manuscript writing, final approval of manuscript, financial support, administrative support; A.G.T.: conception and design, provision of study material, manuscript writing, final approval of manuscript.

## DISCLOSURES OF POTENTIAL CONFLICTS OF INTEREST

The authors indicate no potential conflicts of interest.

## REFERENCES

- Dragun D, Hoff U, Park JK et al. Ischemia-reperfusion injury in renal transplantation is independent of the immunologic background. *Kidney Int* 2000;58:2166–2177.
- Eltzschig HK, Eckle T. Ischemia and reperfusion—from mechanism to translation. *Nat Med* 2011;17:1391–1401.
- Cicco G, Panzera PC, Catalano G et al. Microcirculation and reperfusion injury in organ transplantation. *Adv Exp Med Biol* 2005;566:363–373.
- Basile DP. The endothelial cell in ischemic acute kidney injury: Implications for acute and chronic function. *Kidney Int* 2007;72:151–156.
- Basile DP. Rarefaction of peritubular capillaries following ischemic acute renal failure: A potential factor predisposing to progressive nephropathy. *Curr Opin Nephrol Hypertens* 2004;13:1–7.
- Metcalfe MS, Butterworth PC, White SA et al. A case-control comparison of the results of renal transplantation from heart-beating and non-heart-beating donors. *Transplantation* 2001;71:1556–1559.
- Koffman G, Gambaro G. Renal transplantation from non-heart-beating donors: A review of the European experience. *J Nephrol* 2003;16:334–341.
- Reinders ME, de Fijter JW, Roelofs H et al. Autologous bone marrow-derived mesenchymal stromal cells for the treatment of allograft rejection after renal transplantation: Results of a phase I study. *STEM CELLS TRANSLATIONAL MEDICINE* 2013;2:107–111.
- Ren G, Chen X, Dong F et al. Concise review: Mesenchymal stem cells and translational medicine: Emerging issues. *STEM CELLS TRANSLATIONAL MEDICINE* 2012;1:51–58.
- Giraud S, Favreau F, Chatauret N et al. Contribution of large pig for renal ischemia-reperfusion and transplantation studies: The preclinical model. *J Biomed Biotechnol* 2011;532127.
- Perin L, Giuliani S, Jin D et al. Renal differentiation of amniotic fluid stem cells. *Cell Prolif* 2007;40:936–948.
- De Coppi P, Bartsch G Jr., Siddiqui MM et al. Isolation of amniotic stem cell lines with potential for therapy. *Nat Biotechnol* 2007;25:100–106.
- In 't Anker PS, Scherjon SA, Kleijburg-van der Keur C et al. Isolation of mesenchymal stem cells of fetal or maternal origin from human placenta. *STEM CELLS* 2004;22:1338–1345.
- Perin L, Sedrakyan S, Giuliani S et al. Protective effect of human amniotic fluid stem cells in an immunodeficient mouse model of acute tubular necrosis. *PLoS One* 2010;5:e9357.
- Hauser PV, De Fazio R, Bruno S et al. Stem cells derived from human amniotic fluid contribute to acute kidney injury recovery. *Am J Pathol* 2010;177:2011–2021.
- Sedrakyan S, Da Sacco S, Milanese A et al. Injection of amniotic fluid stem cells delays progression of renal fibrosis. *J Am Soc Nephrol* 2012;23:661–673.
- Jayle C, Favreau F, Zhang K et al. Comparison of protective effects of trimetazidine against experimental warm ischemia of different durations: Early and long-term effects in

a pig kidney model. *Am J Physiol Renal Physiol* 2007;292:F1082–F1093.

**18** Rossard L, Favreau F, Demars J et al. Evaluation of early regenerative processes in a pre-clinical pig model of acute kidney injury. *Curr Mol Med* 2012;12:502–505.

**19** Chen J, Lu Z, Cheng D et al. Isolation and characterization of porcine amniotic fluid-derived multipotent stem cells. *PLoS One* 2011;6:e19964.

**20** Bottai D, Cigognini D, Nicora E et al. Third trimester amniotic fluid cells with the capacity to develop neural phenotypes and with heterogeneity among sub-populations. *Restor Neurol Neurosci* 2012;30:55–68.

**21** Skardal A, Mack D, Kapetanovic E et al. Bioprinted amniotic fluid-derived stem cells accelerate healing of large skin wounds. *STEM CELLS TRANSLATIONAL MEDICINE* 2012;1:792–802.

**22** Zhang P, Baxter J, Vinod K et al. Endothelial differentiation of amniotic fluid-derived stem cells: Synergism of biochemical and shear force stimuli. *Stem Cells Dev* 2009;18:1299–1308.

**23** Da Sacco S, Sedrakyan S, Boldrin F et al. Human amniotic fluid as a potential new source of organ specific precursor cells for future regenerative medicine applications. *J Urol* 2010;183:1193–1200.

**24** Dominici M, Le Blanc K, Mueller I et al. Minimal criteria for defining multipotent mesenchymal stromal cells. The International Society for Cellular Therapy position statement. *Cytotherapy* 2006;8:315–317.

**25** Bai J, Wang Y, Liu L et al. Human amniotic fluid-derived c-kit(+) and c-kit(-) stem cells:

Growth characteristics and some differentiation potential capacities comparison. *Cytotechnology* 2012;64:577–589.

**26** Van Raemdonck D, Neyrinck A, Rega F et al. Machine perfusion in organ transplantation: A tool for ex-vivo graft conditioning with mesenchymal stem cells? *Curr Opin Organ Transplant* 2013;18:24–33.

**27** Anders HJ, Vielhauer V, Schlöndorff D. Chemokines and chemokine receptors are involved in the resolution or progression of renal disease. *Kidney Int* 2003;63:401–415.

**28** Pescovitz MD, Lunney JK, Sachs DH. Preparation and characterization of monoclonal antibodies reactive with porcine PBL. *J Immunol* 1984;133:368–375.

**29** Banfi A, von Degenfeld G, Blau HM. Critical role of microenvironmental factors in angiogenesis. *Curr Atheroscler Rep* 2005;7:227–234.

**30** Horie N, Pereira MP, Niizuma K et al. Transplanted stem cell-secreted VEGF effects post-stroke recovery, inflammation, and vascular repair. *STEM CELLS* 2011;29:274–285.

**31** Wu Y, Chen L, Scott PG et al. Mesenchymal stem cells enhance wound healing through differentiation and angiogenesis. *STEM CELLS* 2007;25:2648–2659.

**32** Woolf AS, Gnudi L, Long DA. Roles of angiopoietins in kidney development and disease. *J Am Soc Nephrol* 2009;20:239–244.

**33** Autiero M, Waltenberger J, Communi D et al. Role of PlGF in the intra- and intermolecular cross talk between the VEGF receptors Flt1 and Flk1. *Nat Med* 2003;9:936–943.

**34** Luttun A, Tjwa M, Moons L et al. Revascularization of ischemic tissues by PlGF treatment,

and inhibition of tumor angiogenesis, arthritis and atherosclerosis by anti-Flt1. *Nat Med* 2002;8:831–840.

**35** Li XD, Chen J, Ruan CC et al. Vascular endothelial growth factor-induced osteopontin expression mediates vascular inflammation and neointima formation via Flt-1 in adventitial fibroblasts. *Arterioscler Thromb Vasc Biol* 2012;32:2250–2258.

**36** Kasper G, Dankert N, Tuischer J et al. Mesenchymal stem cells regulate angiogenesis according to their mechanical environment. *STEM CELLS* 2007;25:903–910.

**37** van Meeteren LA, ten Dijke P. Regulation of endothelial cell plasticity by TGF- $\beta$ . *Cell Tissue Res* 2012;347:177–186.

**38** Schmidt-Weber CB, Blaser K. Regulation and role of transforming growth factor-beta in immune tolerance induction and inflammation. *Curr Opin Immunol* 2004;16:709–716.

**39** ten Dijke P, Arthur HM. Extracellular control of TGFbeta signalling in vascular development and disease. *Nat Rev Mol Cell Biol* 2007;8:857–869.

**40** Melief SM, Schrama E, Brugman MH et al. Multipotent stromal cells induce human regulatory T cells through a novel pathway involving skewing of monocytes towards anti-inflammatory macrophages. *STEM CELLS* 2013;31:1980–1991.

**41** Fei X, Jiang S, Zhang S et al. Isolation, culture, and identification of amniotic fluid-derived mesenchymal stem cells. *Cell Biochem Biophys* 2013;67:689–694.

**42** Chien KR. Stem cells: Lost in translation. *Nature* 2004;428:607–608.



See [www.StemCellsTM.com](http://www.StemCellsTM.com) for supporting information available online.